Experimental and Analytical Fatigue Data for Notched Shafts in Bending

Ali-Reza Gowhari-Anaraki, Stephen John Hardy and
Mohammad Kazem Pipelzadeh

ABSTRACT

An experimental investigation has been carried out on two types of shaft with different stress concentration features in order to determine the notched members fatigue life in bending. The shafts are made from steel with DIN specification CK45, which is widely used for machinery components. These lives are compared with estimates using the simple notch-stress-strain-conversion rules (e.g., Neuber, Linear) and the strain energy density methods in conjunction with the Coffin-Manson strain-life relationship. The paper demonstrates the simplicity and accuracy of the approach although the predictive capability was found to depend on the magnitude of the elastic stress concentration factor.

Keywords: Fatigue life, Neuber rule, linear rule, Glinka method, stress concentration factor

ABSTRAK

Suatu siasatan uji kaji telah dilakukan terhadap dua jenis aci dengan keadaan penumpuan tegasan yang berbeza bagi menentukan hayat lesu anggota yang bertakuk ketika membengkok. Aci-aci itu diperbuat daripada keluli dengan spesifikasi DIN CK45, yang banyak digunakan dalam komponen mesin. Hayat lesu itu dibandingkan dengan anggaran yang menggunakan aturan penukaran-terikan-tegasan-takukan (cht. Neuber, Linear) dan kaedah ketumpatan tenaga terikan bersama dengan hubungan terikan-hayat Coffin-Manson. Kertas ini menunjukkan kemudahan dan kejituan pendekatan ini walaupun keupayaan ramalan didapati bergantung kepada magnitud faktor penumpuan tegasan kenyal.

Katakunci: Hayat lesu, aturan Neuber, aturan rule, kaedah Glinka, faktor penumpuan tegasan

INTRODUCTION

Many engineering components contain abrupt changes of geometry. These are commonly referred to as 'notches' or 'stress raisers'. These are the main source of crack initiation followed by subsequent propagation and sudden failure under fatigue loading conditions. Designers must consider their potential effects in order to assess the integrity of such components. When a notched component is subjected to an external load, there is a direct relationship between the maximum stress at the notch root and the nominal stress applied remotely from the notch region. The ratio between the

maximum and nominal stress is referred to as the elastic stress concentration factor, K_t. This is valid provided that the maximum stress is below the yield stress of the material. Values of K_t (i.e., experimental and analytical) for a variety of notched components are readily available, e.g., see Pilkey (1997) and Hardy and Malik (1992). These are both geometry and loading dependent and are particularly useful for brittle materials in order to predict the peak stresses. However, for ductile materials, the local region of high stress is relieved as yielding occurs and the maximum stress is no longer equal to K_t multiply by the nominal stress. Therefore, the elastic stress concentration factor is not appropriate and a criterion based on the accumulation of strain is used to assess the fatigue behaviour. This is particularly true when significant yielding occurs and failures are within the low cycle fatigue regime.

The accumulation of strain in a post-yielding situation is not easily determined and mathematical solutions are only available for a relatively small number of specific cases. Non-linear finite element analysis can be used, but the method is expensive and time consuming. Furthermore, the modelling of the cyclic elastic-plastic material behaviour is an area of approximation and one where research continues to be focussed. Alternatively, numerical relationships have been proposed, such as the notch stress-strain conversion (NSSC) rules (Fuchs & Stephens 1980; Neuber 1961) and strain energy density methods (Glinka & Nowack 1988) to estimate these strain values.

Analytical relationships to predict the strain range at a notch have been proposed by various researchers. Crews and Hardrath (1966) conducted experimental investigations into the plastic stresses at the root of a notched plate made from aluminium alloy with $K_t = 2$. The component was subjected to repeated cyclic tension loading. The fatigue life was determined using the *S-N* diagram. The authors developed a correlation for the notched stresses and this provided accurate fatigue life predictions. Topper et al. (1969) conducted experimental investigations on aluminium plates subjected to reverse loading in order to predict the life of the notched components, with K_t in the range 2 to 4. They compared their results with estimates using Neuber's rule (Neuber 1961) and these were found to be in good agreement. Papirno, 1971 compared Neuber &d Hardrath-Ohman rules (Hardrath & Ohman, 1953) with measurements made on notched tensile steel strips under monotonically increasing load with large strains. He concluded that for K_t between 1.5 and 2, Neuber's rule provided more accurate estimates than Hardrath-Ohman's rule. However, the estimates coincided when $K_t = 2.5$. Kotani et al., 1976 conducted experimental tests on two types of notched specimens, i.e., side notched plates and circumferential notched round bars, to study the cyclic stress-strain behaviour. The notched plate results were in good agreement with estimates using Neuber's rule, whereas, the notched bar results were significantly lower than the estimates. Other investigations into the suitability and accuracy of the NSSC rule estimates include the work of Byre-Gowda and Topper (1970) on flat plates with circular and elliptical holes, Hoffman and Seeger (1985) on round bars with deep circumferential notches, Conel and Nowack (1977) on flat plates with key-holes and Wang (1990) on U- and V-notched specimens.

In this investigation, two types of notched components have been considered; stepped shafts with K_t values of 1.35 and 2.2 and grooved shafts with K_t values of 1.6 and 2.6, as shown in Figure 1. These components are subjected to bending loads. The experimental results of nominal stress range (S_a) against number of stress reversals to failure $(2N_f)$ are compared with NSSC rule estimates and values obtained using strain energy density theory. Although the monotonic and cyclic material parameters required by these estimation methods are well documented, the paper describes how they have been obtained from simple monotonic and cyclic push-pull tests (using the two un-notched components shown in Figure 2), since such data is not readily available for all materials.
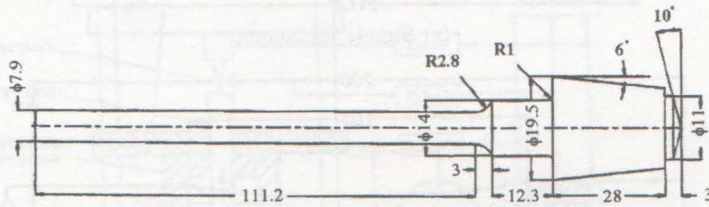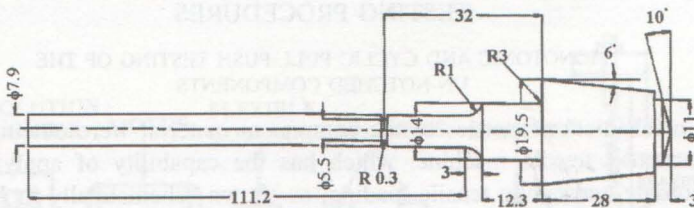

Geometry 1-   Stepped shaft with K_t =1.35
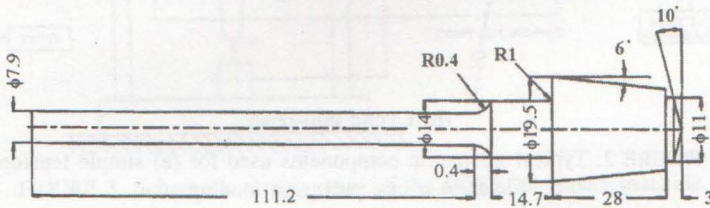
Geometry 2-   Stepped shaft with K_t =2.2
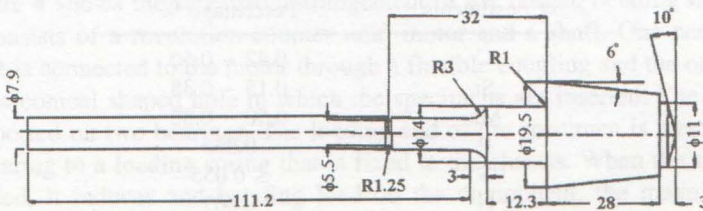
Geometry 3-   Grooved shaft with K_t =1.6

Geometry 4-   Grooved shaft with K_t =2.6

FIGURE 1. Notched component geometries

COMPONENT MATERIAL

The components were made from steel with DIN specification CK45, which is often used for machine parts, in particular in the manufacture of nuts and bolts. The main constituents are shown in Table 1.
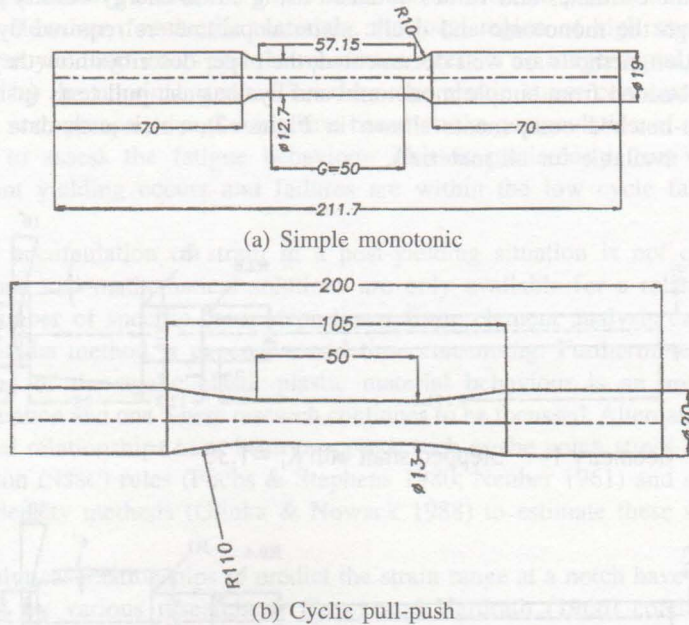

(a) Simple monotonic

(b) Cyclic pull-push

FIGURE 2. Typical geometric components used for (a) simple tension and (b) cyclic pull-push loading

TABLE 1. Components' material analysis

Constituents	Percentage %
C	0.42 ~ 0.50
Si	0.15 ~ 0.35
Mn	0.50 ~ 0.80
P	0.035
S	≤ 0.035
N	0.007

TESTING PROCEDURES

MONOTONIC AND CYCLIC PULL-PUSH TESTING OF THE UN-NOTCHED COMPONENTS

The mechanical properties of the component material were obtained using an INSTRON tensile machine, which has the capability of applying both monotonic and cyclic tensile loading, as shown schematically in Figure 3. The machine comprises of two main elements, the mechanical parts and the electronics. The mechanical parts consist of a pump and piston for the movement of the mounted jaw. This is operated by a hydraulic system using pressurised oil. The jaws can accommodate flat and round components with

various dimensions. The electronic control consists of a computer for monitoring, instructing and measuring the movements. The machine uses an extensometer to measure the deformation within a gauge length. The dimensions of the test components are in accordance with the appropriate standards, e.g., see Dowling (1999). Tests were carried out under strain controlled axial loading. In all cases, the material exhibits cyclic strain hardening. Also, a stabilized loop was reached within a maximum of 20 cycles.
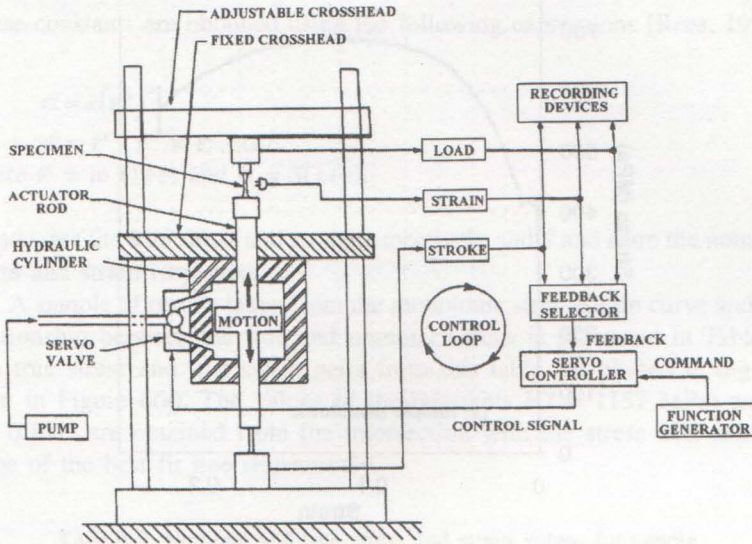
FIGURE 3. Schematic arrangement of the INSTRON tensile machine.

CYCLIC BEND TESTING OF THE NOTCHED COMPONENTS

Figure 4 shows the schematic arrangement of the fatigue bending machine. It consists of a revolution counter unit, motor and a shaft. One end of the shaft is connected to the motor through a flexible coupling and the other end has a conical shaped hole in which the specimens are inserted. The shaft is supported on two bearings. The loading end of the specimen is attached via a bearing to a loading spring that is fixed to the chassis. When the spring is loaded, it induces and bending load on the component, the magnitude of which is indicated. Upon the failure of the component, a cut-off device stops the entire system. The motor rotates at a maximum speed of 3000 rpm.
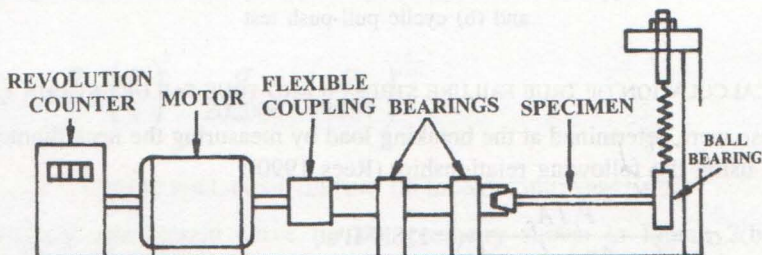
FIGURE 4. Schematic arrangement of the fatigue bending machine

MONOTONIC TENSILE TESTING OF UN-NOTCHED SPECIMENS

A typical stress-strain curve for the geometry shown in Figure 2(a) is presented in Figure 5(a). The following material properties were obtained:

$$(\sigma_y)_{\text{upper}} = 425 \text{ MPa}, \qquad (\sigma_y)_{\text{lower}} = 410 \text{ MPa},$$
$$E = 202 \text{ GPa}, \qquad S_u = 683.7 \text{ MPa}.$$
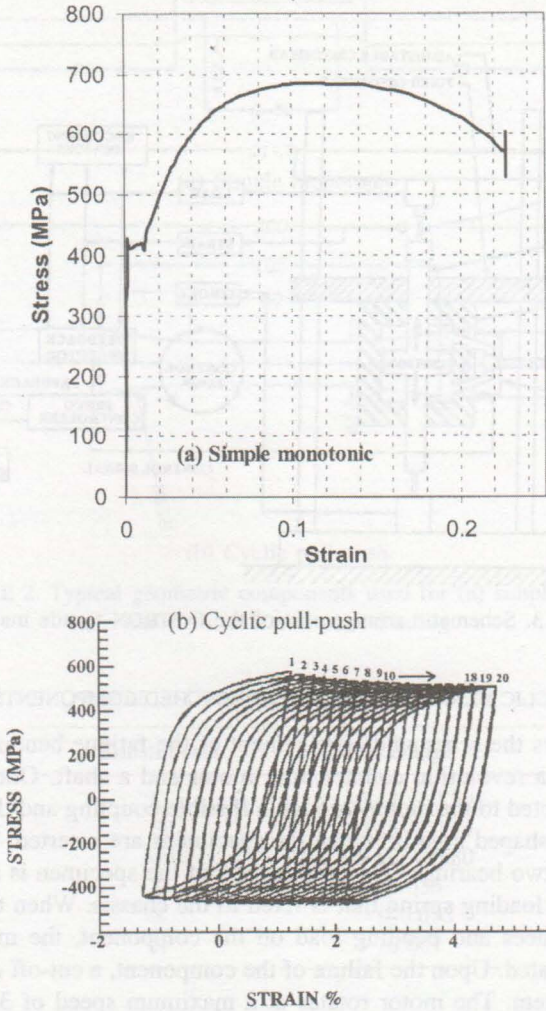
FIGURE 5. Typical stress-strain curve for (a) simple monotonic loading and (b) cyclic pull-push test

CALCULATION OF TRUE FAILURE STRESS σ_f AND TRUE FAILURE STRAIN ε_f

These were determined at the breaking load by measuring the neck diameter and using the following relationships (Rees 1990):

$$\sigma_f = \frac{P_f / A_f}{\left(1 + \dfrac{4r}{d}\right) \ln\left(1 + \dfrac{d}{4r}\right)} = 1188 \text{MPa}, \tag{1}$$

and $\quad \varepsilon_f = \ln\left(\dfrac{A_o}{A_f}\right) = \ln\left(\dfrac{100\%}{100\% - RA\%}\right) = 0.689$, $\hfill$ (2)

where $RA\% = \left(\dfrac{A_o - A_f}{A_f}\right) \times 100\% = 49.78\%$.

CALCULATION OF STRENGTH FACTOR k AND STRAIN HARDENING INDEX n

These constants are obtained using the following expressions [Rees, 1990]:

$$\sigma = k\left(\varepsilon^{pl}\right)^n,$$ (3)

and $\quad \varepsilon^{pl} = \varepsilon^t - \varepsilon^{el} = \varepsilon^t - \sigma/E,$ $\hfill$ (4)

where $\varepsilon^t = \ln(1+e)$ and $\sigma = S(1+e)$.

σ and ε are the true stress and strain respectively and S and e are the nominal stress and strain respectively.

A sample of results taken from the monotonic stress-strain curve and the relationship between the true and nominal values is presented in Table 2. The true stress and true strain pairs from this table are plotted in log-log form in Figure 6(a). The values of the constants k (= 1157 MPa) and n (= 0.191) are obtained from the intersection with the stress axis and the slope of the best fit line respectively.

TABLE 2. Nominal and true stress and strain values for simple monotonic loading test

e^t	S (MPa)	e^t	s (MPa)	s/E	e^{pl}
0.005	413.1	0.0050	415.1	0.0021	0.0029
0.010	427.0	0.0010	431.3	0.0021	0.0079
0.002	480.0	0.0198	489.6	0.0024	0.0174
0.025	525.0	0.0247	538.1	0.0027	0.0220
0.035	583.9	0.0344	604.3	0.0030	0.0314
0.060	650.8	0.0583	689.8	0.0034	0.0549
0.080	672.1	0.0770	725.7	0.0036	0.0734
0.110	682.8	0.1043	757.9	0.0038	0.1005

Hence the Ramberg-Osgood monotonic equation (Ramberg & Osgood, 1943) becomes:

$$\varepsilon = \frac{\sigma}{E} + \left(\frac{\sigma}{k}\right)^{\frac{1}{n}} = \frac{\sigma}{202000} + \left(\frac{\sigma}{1157}\right)^{\frac{1}{0.191}}.$$ (5)

CYCLIC PULL-PUSH TESTING OF UN-NOTCHED SPECIMENS

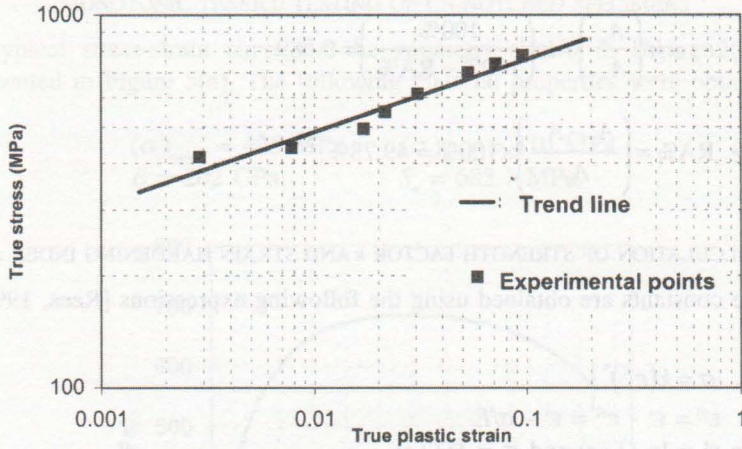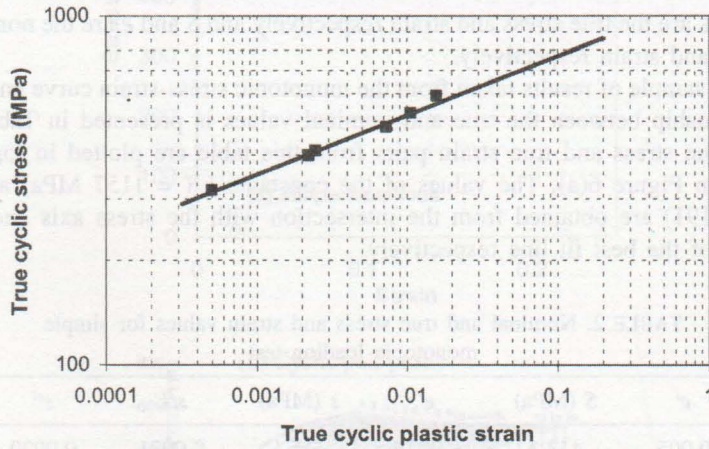A typical stress-strain curve for the geometry shown in Figure 2(b) is presented in Figure 5(b).

(a) Simple tension: $n= 191$ and $k= 1157$

(b) Cyclic pull-push loading: $n' = 172$ and $k' = 1144$

FIGURE 6. Typical true stress-true strain for (a) simple tension
and (b) cyclic pull-push loading

CALCULATION OF CYCLIC STRENGTH FACTOR k' AND CYCLIC STRAIN HARDENING INDEX n'

For cyclic loading, stress and strain ranges are used and hence Equation (4) is rewritten as:

$$\varepsilon_a^{pl} = \varepsilon_a^t - \varepsilon_a^{el}, \tag{6}$$

where $\varepsilon_a^t = \ln(1+e_a)$ and $\sigma_a = S_a(1+e_a)$.

σ_a and ε_a are the true stress and strain range respectively and S_a and e_a are the nominal stress and strain range respectively.

The values of the constants k' ($= 1144$ MPa) and n' ($= 0.172$) are obtained in similar way to that described in Section 4.2, using sample data from Table 3 plotted in log-log form as shown in Figure 6(b). Hence the Ramberg-Osgood cyclic equation (Ramberg & Osgood 1943) becomes:

$$\varepsilon_a = \frac{\sigma_a}{E} + \left(\frac{\sigma_a}{k}\right)^{\frac{1}{n'}} = \frac{\sigma_a}{202000} + \left(\frac{\sigma_a}{1144}\right)^{\frac{1}{0.172}}. \tag{7}$$

TABLE 3. Nominal and true stress and strain values for cyclic pull-push loading test

e_a^t	S_a (MPa)	e_a^t	s_a (MPa)	s_a/E	e_a^{pl}
0.0016	307.1	0.0016	307.5	0.0015	0.0000
0.0020	312.7	0.0020	313.0	0.0015	0.0005
0.0042	393.0	0.0042	394.7	0.0020	0.0022
0.0045	400.0	0.0042	401.8	0.0020	0.0024
0.0097	471.5	0.0096	476.1	0.0024	0.0072
0.0131	522.0	0.0130	528.8	0.0026	0.0104
0.0187	570.0	0.0185	580.7	0.0029	0.0156

FATIGUE TESTING OF THE NOTCHED COMPONENTS DETERMINATION OF K_f

For a component with a high notch sensitivity, K_f approaches K_t. However, if it is not sensitive to the notch, K_f approaches unity. Hence, the sensitivity, q, is the indication of the deviation between K_t and K_f which are related by:

$$K_f = 1 + q(K_t - 1). \tag{8}$$

Peterson (Pilkey 1997) experimentally obtained an expression for q as:

$$q = \frac{1}{1 + \frac{\alpha}{\rho}}, \tag{9}$$

where ρ is the notch radius and a is a material property which depends on the ultimate tensile strength of the component material, S_u. For $S_u \geq 550$ MPa under axial and bending loading, $\alpha = 0.025(2070/S_u)^{1.8} = 0.184$.

Table 4 presents the predicted values of K_t and K_f for the range of geometries considered. Geometries 3 and 4 contain two notches, i.e., the blend fillet and the grooves. The dimensions and positions of these notches were designed in such a way that the maximum elastic stress in the groove is 3 times greater than in the fillet. Also, the principle of St. Venant's is observed in that a uniform stress distribution is achieved between the two

TABLE 4. Values of K_t and K_f for the range of geometries considered

Geometry	K_t	K_f
1	1.35	1.33
2	2.2	1.82
3	1.6	1.52
4	2.6	2

notches (Gowhari-Anaraki et al. 2000). The inclusion of the fillet in the above components is strictly for the safety (protection) of the machine.

COMPONENT FATIGUE LIVES

The results from the experimental fatigue tests are presented in Table 5 in the form of S_a-$2N_f$ pairs for the four geometries.

TABLE 5. Experimental fatigue test results

Geometry	S_a (MPa)	$2N_f$
1	263.9	2,864,800
	274.6	575,740*
	295.6	580,220
	337.8	86,440
	358.9	64,500
	422.2	26,520
2	180.0	2,134,410
	232.7	502,450
	296.2	130,220
	335.5	47,400
	359.7	30,120
	423.1	11,560
3	220.4	5,358,760
	236.2	1,012,740
	288.6	331,420
	314.9	199,300
	341.1	50,300*
	367.4	54,440
	393.6	21,640
4	186.0	643,260
	223.0	489,520
	239.0	425,120
	265.5	262,400
	292.0	182,840
	318.6	45,600
	345.1	35,740
	398.2	19,210

* Possible surface scratch or metallurgical defect

DEVELOPMENT OF S_a-$2N_f$ CURVES BASED ON LINEAR, NEUBER AND STRAIN ENERGY DENSITY METHODS

The low cycle fatigue life of a notched component can be estimated from the Coffin-Manson equation:

$$\varepsilon_a = \frac{\sigma_f'}{E}\left(2N_f\right)^b + \varepsilon_f'\left(2N_f\right)^c. \tag{10}$$

The material properties in Equation (10) have been obtained from the tests described in Sections 4 and 5, i.e.:

$\sigma'_f \cong s_f = 1188$ MPa
$E = 202$ GPa
$\varepsilon'_f \cong \varepsilon_f = 0.689$
$b = -n'/(1+5n') = -0.172/(1+5 \times 0.172) = -0.0925$
$c = b/n' = -0.0925/0.172 = -0.538$.

Hence, the Coffin-Manson equation, for this material, becomes:

$$\varepsilon_a = 0.0059 \left(2N_f\right)^{-0.0925} + 0.689 \left(2N_f\right)^{-0.538}. \qquad (11)$$

Because the experimental results are based on the nominal applied stress range, S_a, it is necessary, for comparative purposes to re-write Equation (11) in terms of S_a. The relationship between ε_a and S_a depends on the selected NSSC rule or method.

LINEAR RULE (Fuchs & Stephens, 1980)

For the linear rule, it is assumed that the elastic stress concentration factor, K_t, is equal to the elastic-plastic strain concentration factor, K_ε, and the relationship between ε_a and S_a thus becomes:

$$S_a = E \, \varepsilon_a / K_t. \qquad (12)$$

Consequently, the specific Coffin-Manson equation is re-written as:

$$S_a = \frac{202000}{K_t} \left[0.0059 \left(2N_f\right)^{-0.0925} + 0.689 \left(2N_f\right)^{-0.538} \right]. \qquad (13)$$

NEUBER RULE (Neuber, 1961)

For the Neuber rule, the relationship between the elastic stress concentration factor, K_t, the plastic stress concentration factor, K_σ, and the elastic-plastic strain concentration factor, K_ε, is:

$$K_t^2 = K_s \cdot K_e, \qquad (14)$$

from which, the relationship between ε_a and S_a becomes:

$$S_a = \sqrt{\left(\varepsilon_a \cdot \sigma_a\right) \frac{E}{K_t^2}}, \qquad (15)$$

where the true stress range, σ_a, is calculated from Equation (7). In this case, the solution is not direct and the following procedure is adopted in order to obtain pairs of $(S_a, 2N_f)$ values:
1. Select a value for $2N_f$ and obtain ε_a from Equation (11)
2. Calculate the corresponding value of σ_a from Equation (7)
3. Determine the corresponding value of S_a from Equation (15) with $E = 202$ GPa

STRAIN ENERGY DENSITY (GLINKA) METHOD (Glinka & Nowack, 1988)

The nominal stress range, S_a using strain energy density theory, is expressed as:

$$\frac{\left(K_t \cdot S_a\right)^2}{2E} = \frac{\sigma_a^2}{2E} + \left(\frac{\sigma_a}{n'+1}\right)\left(\frac{\sigma_a}{k'}\right)^{\frac{1}{n'}} \quad (16)$$

Here, procedure to obtain pairs of $(S_a, 2N_f)$ values is the same as for the Neuber rule, with the exception that S_a is obtained from Equation (16) with $n' = 0.172$, $k' = 1144$ MPa and $E = 202000$ MPa.

DEVELOPMENT OF S_a-$2N_f$ CURVES BASED ON EXPERIMENTALLY-DERIVED MATERIAL DATA

The theoretical high cycle fatigue life of the un-notched components is given by Fuchs and Stephens (Fuchs & Stephens, 1980):

$$S_a = \sigma_f' \left(2N_f\right)^{b'}, \quad (17)$$

where b' and s_f' are material constants and can be derived from the elastic strain-life diagram obtained from pull-push tests on un-notched specimens. Equation (17) has been modified for notched specimens:

$$S_a = A \left(2N_f\right)^{B}, \quad (18)$$

where A and B can be found from two distinct points on the S_a-$2N_f$ diagram:
   (i) $S_a = \sigma_f'$ when $2N_f = \frac{1}{2}$
and (ii) $S_a = S_f/K_f$ when $2N_f = 10^7$
where S_f is the endurance limit of the material.

In this paper, it is assumed that $S_f = S_u/2 = 341.85$ MPa (Shigley & Mischke, 1989) and $\sigma_f' = \sigma_f (= 1188$ MPa). Hence, for the components considered, Equation (18) becomes:

Geometry 1 $S_a = 1115 (2N_f)^{-0.091}$ (19)
Geometry 2 $S_a = 1100 (2N_f)^{-0.11}$ (20)
Geometry 3 $S_a = 1109 (2N_f)^{-0.099}$ (21)
Geometry 4 $S_a = 1097 (2N_f)^{-0.115}$ (22)

RESULTS AND DISCUSSION

The $(S_a$-$2N_f)$ relationships obtained using the above methods, together with the experimental results are presented in Figures 7 to 10 for Geometries 1 to 4, respectively.

For the techniques based on a low cycle fatigue assumption, the linear method provides the greatest fatigue life estimate for any nominal stress range, followed by the strain energy density method estimate and then the
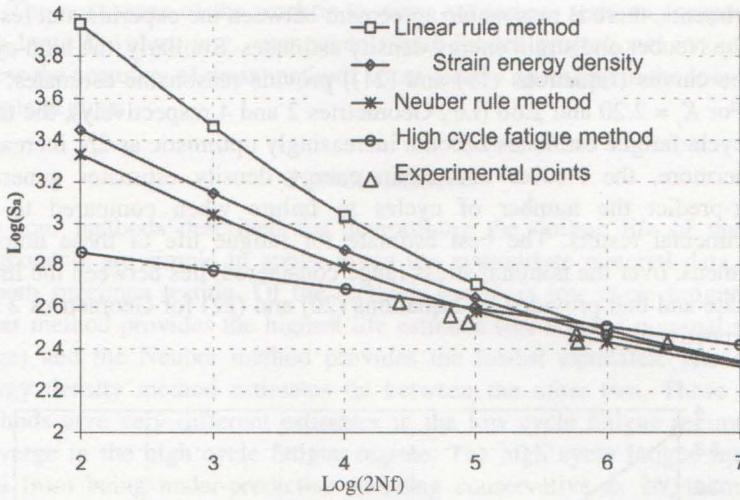
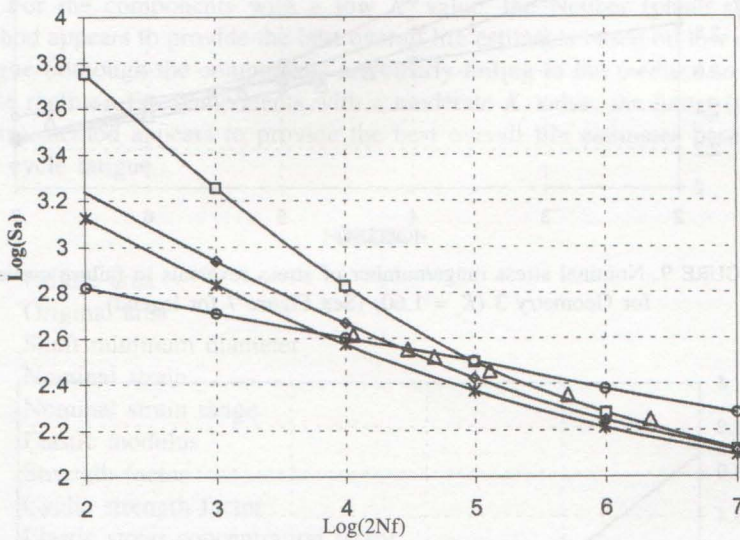FIGURE 7. Nominal stress range/number of stress reversals to failure curve for Geometry 1 ($K_t = 1.36$)

FIGURE 8. Nominal stress range/number of stress reversals to failure curve for Geometry 2 ($K_t = 2.20$) (See Figure 7 for legend)

estimate using the Neuber rule. The S_a-$2N_f$ high cycle fatigue curve derived from the material smooth-specimen data provides the greatest life estimate for large $2N_f$ values and the lowest life estimate for low $2N_f$ values. The cross-over point is K_t dependent.

For $K_t = 1.36$ and 1.60 (i.e. Geometries 1 and 3 respectively), the linear and strain energy density methods generally provide conservative estimates when compared with the experimental results for the notched specimens, particularly as $2N_f$ reduces. Similarly, the Neuber estimates become increasingly conservative as one moves from the high cycle to the low cycle regime. Nevertheless, over the nominal stress ranges covered in the

28

experiments, there is reasonable agreement between the experimental results and the Neuber and strain energy density estimates. Similarly, the high cycle fatigue curves (Equations (19) and (21)) provide reasonable estimates.

For $K_t = 2.20$ and 2.60 (i.e., Geometries 2 and 4 respectively), the three low cycle fatigue estimates become increasingly optimistic as $2N_f$ increases. Furthermore, the Neuber and strain energy density estimates generally under-predict the number of cycles to failure when compared to the experimental results. The best estimate for fatigue life of these notched specimens, over the nominal stress range considered, lies between the linear estimate and that provided by Equations (20) and (22) for Geometries 2 and 4, respectively.
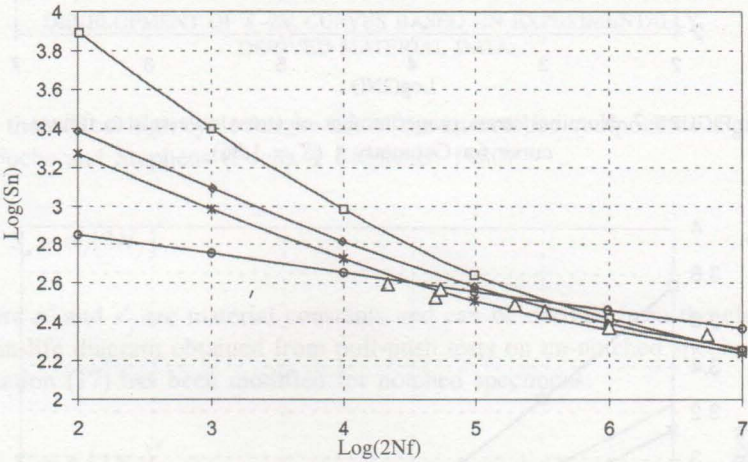
FIGURE 9. Nominal stress range/number of stress reversals to failure curve for Geometry 3 ($K_t = 1.60$) (See Figure 7 for legend)
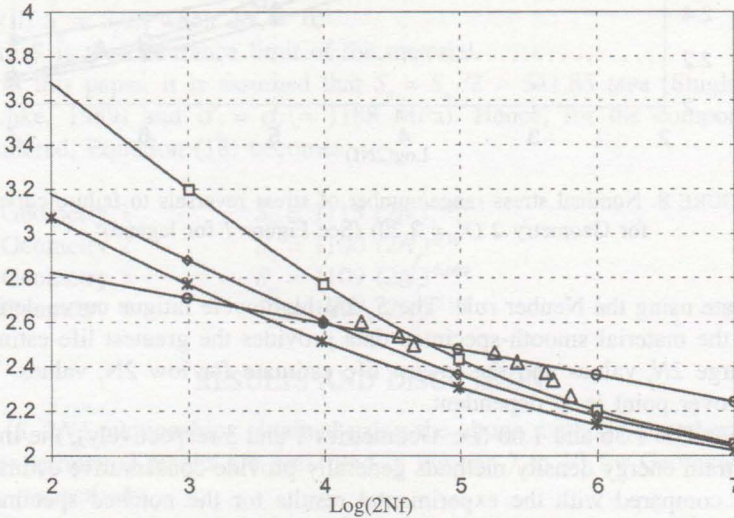
FIGURE 10. Nominal stress range/number of stress reversals to failure curve for Geometry 4 ($K_t = 2.60$) (See Figure 7 for legend)

The next stage of the work is to carry out fatigue tests on components with large K_t values (e.g., components with loaded projections) in order to assess the accuracy of these methods when clearly operating in the low cycle fatigue regime.

CONCLUSIONS

The four methods described for determining the fatigue life of notched components are simple to apply, given the appropriate material data from smooth specimen testing. Of the methods based on low cycle fatigue, the linear method provides the highest life estimate (for a given nominal stress range) and the Neuber method provides the lowest estimates. The strain energy density method estimates lie between the other two. These three methods give very different estimates in the low cycle fatigue regime but converge in the high cycle fatigue regime. The high cycle fatigue method goes from being under-predictive to being conservative as $2N_f$ increases. Over the range of bending loads considered in the experiments, reasonable accuracy can be achieved. The choice of 'best estimate' is both K_t and S_a dependent.

For the components with a low K_t value, the Neuber (plane stress) method appears to provide the best overall life estimates based on low cycle fatigue (although the components are clearly failing in the medium to high cycle regime). For components with a moderate K_t value, the linear (plane strain) method appears to provide the best overall life estimates based on low cycle fatigue.

NOTATION

A_f Failure area
A_o Original area
d Shaft minimum diameter
e Nominal strain
e_a Nominal strain range
E Elastic modulus
k Strength factor
k' Cyclic strength factor
K_t Elastic stress concentration factor
K_f Fatigue strength factor
n Strain hardening index
n' Cyclic strain hardening index
N_f Number of cycles to failure (i.e., fatigue life)
$2N_f$ Number of load reversals to failure
P_f Final applied load
q Notch sensitivity factor
r Necking radius
RA Reduction in area
S Nominal stress
S_a Nominal stress range
S_u Ultimate tensile strength
α Material property

ε True strain (at the notch)

ε_a True strain range (at the notch)

ε_f True failure strain (at the notch)

ρ Notch radius

σ True stress (at the notch)

σ_a True stress range (at the notch)

σ_f True failure stress

σ_y Yield stress

Superscripts

el   Elastic

pl   Plastic

t   Total

REFERENCES

Byre-Gowda, C. V. and Topper, T. H. 1970. On the relation between stress and strain concentration factors in notched members in plane stress. *ASME J Appl. Mech.* 37: 77-84.

Conel, A. and Nowack, H. 1977. Verification of Neuber-based notch analysis by the companion-specimen method. *J. Exp. Mech.* 17: 57-63.

Crews, J. H. and Hardrath, H. F. 1966. A study of cyclic plastic stresses at the notch root. *J. Exp. Mech.* 6: 313-320.

Dowling, N. E. 1999. *Mechanical behaviour of materials: Engineering methods for deformation, fracture, and fatigue.* Upper Saddle River: Prentice Hall.

Fuchs, H.O. and Stephens, R. I. 1980. *Metal fatigue in engineering.* New York: John Wiley.

Glinka, G. and Nowack, H. 1988. Elastic plastic plane strain analysis of stress and strain at the notch root. *J. Eng Mater. Tech.* 110: 195-204.

Gowhari-Anaraki, A. R., Pipelzadeh, M. K. and Hardy S. J. 2000. Improving the life of joint-welded components with stress concentrations using Saint Venant's principle. *Proc. 9th Congress of Chilian Mechanical Engineering.* Universidad Tecnica Federico Santa Maria, Valparaiso, Chile, p. 144.

Hardrath, H. F. and Ohman, L., 1953. A study of elastic and plastic stress concentration factors due to notches and fillets in flat plates. *NACA report 1117.*

Hardy, S. J. and Malik, N. H. 1992. A survey of post-Peterson stress concentration factor data. *Int. J. Fatigue* 14(3): 147-153.

Hoffman, M. and Seeger, T. 1985. A generalized method for estimating multiaxial elastic plastic notch stress and strain *J. Eng. Mater. Tech.* 107: 250-260.

Kotani, S., Koibushi, K. and Kasai, K. 1976. The effect of notches on cyclic stress strain behaviour and fatigue crack initiation. *Proc. Conf. Mechanical Behaviour of Materials.* Boston, USA.

Neuber, H. 1961. Theory of stress concentration for shear strained prismatical bodies with arbitrary non-linear stress-strain law. *J. Appl. Mech.* 28: 544-550.

Papirno, R. 1971. Plastic stress strain history at notch roots in tensile strips under monotonic loading. *J. Exp. Mech.* 11: 446-452.

Pilkey, W.D., 1997, *Peterson's Stress Concentration Factors.* 2nd edition. New York: John Wiley & Sons.

Ramberg, G. and Osgood, W. R. 1943. Description of stress strain curve by three parameters. *NACA Tech Note 902.*

Rees, D. A. W. 1990. *The mechanics of solids and structures.* London: McGraw-Hill.

Shigley, J.E. & Mischke, C.R. 1989. *Mechanical Engineering Design.* 5th edition, New York: McGraw-Hill International Edition.

Topper, T., Wetzel, R. and Morrow, J. 1969. Neuber rule applied to fatigue on notched specimens. *J. Mater LMLSA* 4: 200-209.

Wang, K. C. 1990. An experimental study of notch constraints in low cycle fatigue. PhD. Thesis, The John Hopkins University, USA.

Ali-Reza Gowhari-Anaraki
Department of Mechanical Engineering
Iran University of Science & Technology
Narmak, Tehran
Iran

Stephen John Hardy and Mohammad Kazem Pipelzadeh
School of Engineering, University of Wales-Swansea
Singleton Park, Swansea, SA2 8PP
United Kingdom